nature chemical biology

ARTICLE

PUBLISHED ONLINE: 11 DECEMBER 2017 | DOI: 10.1038/NCHEMBIO.2534

Inhibiting mitochondrial phosphate transport as an unexploited antifungal strategy

Catherine A McLellan[1,2,10], Benjamin M Vincent[1,3,8,10], Norma V Solis[4], Alex K Lancaster[1,8], Lucas B Sullivan[5], Cathy L Hartland[6,8], Willmen Youngsaye[6,8], Scott G Filler[4,7], Luke Whitesell[1,8*] & Susan Lindquist[1,2,9]

The development of effective antifungal therapeutics remains a formidable challenge because of the close evolutionary relationship between humans and fungi. Mitochondrial function may present an exploitable vulnerability because of its differential utilization in fungi and its pivotal roles in fungal morphogenesis, virulence, and drug resistance already demonstrated by others. We now report mechanistic characterization of ML316, a thiohydantoin that kills drug-resistant *Candida* species at nanomolar concentrations through fungal-selective inhibition of the mitochondrial phosphate carrier Mir1. Using genetic, biochemical, and metabolomic approaches, we established ML316 as the first Mir1 inhibitor. Inhibition of Mir1 by ML316 in respiring yeast diminished mitochondrial oxygen consumption, resulting in an unusual metabolic catastrophe marked by citrate accumulation and death. In a mouse model of azole-resistant oropharyngeal candidiasis, ML316 reduced fungal burden and enhanced azole activity. Targeting Mir1 could provide a new, much-needed therapeutic strategy to address the rapidly rising burden of drug-resistant fungal infection.

A health crisis from fungal diseases is looming, as there is a marked increase in at-risk populations and a rising prevalence of drug resistance. The limited number of antifungal classes available and the unacceptably high mortality rate from invasive infections make the need for new antifungals dire. Fungi are eukaryotes, and as such share many conserved proteins and processes with humans, which presents a daunting challenge for the development of new, mechanistically distinct antifungals[1,2]. With this challenge in mind, we executed a high-throughput phenotypic screen for compounds that could reverse resistance to the widely used antifungal fluconazole in a clinical isolate of *Candida albicans* (National Center for Biotechnology Information. PubChem Bioassay Database; AID 2007, https://pubchem.ncbi.nlm.nih.gov/bioassay/2007). A particularly intriguing hit to emerge from this screen was a thiohydantoin (PubChem CID 3889161), which exerted potent antifungal activity as a single agent with no apparent toxicity to mammalian cells. Substructure searches did not reveal any assay interference alerts[3]. Its thiohydantoin core is present in enzalutamide, an androgen-receptor antagonist used in the treatment of prostate cancer[4]. Follow-up synthesis and testing of 51 analogs in a limited SAR study yielded the designated probe compound ML316, a *para*-fluoro phenyl derivative with improved potency and selectivity[5].

The promising attributes of ML316 encouraged further investigation, and we now report discovery of its molecular mechanism of action through a combination of genetic and biochemical approaches. This drug-like compound, distinct from all previously characterized mitochondrial poisons, selectively inhibits Mir1, the major mitochondrial phosphate carrier protein (P_iC). Mir1 transports inorganic phosphate into the inner matrix of fungal mitochondria, where it is used by ATP synthase to generate ATP. Guided by this insight, we used the compound as a probe to investigate the surprising biological consequences of disrupting fungal respiration at its terminal step and to explore the translational therapeutic potential of inhibiting Mir1 in culture and in mice.

RESULTS

ML316 is fungicidal under respiratory conditions

As previously reported[5], ML316 (**1**) exhibited more potent antifungal activity against azole-resistant *C. albicans* than our original screen hit (**2**), whereas substitution of oxygen for sulfur in the thiohydantoin core (**3**) greatly diminished activity (**Fig. 1a**). Although ML316 was equally effective at inhibiting the growth of wild-type *C. albicans* in media with either glucose or nonfermentable glycerol as the sole carbon source, it only inhibited growth of the model fungal organism, *Saccharomyces cerevisiae*, when it was grown in glycerol to enforce respiration (**Fig. 1b**). *C. albicans* is a facultative aerobe and respires when oxygen is present, regardless of the carbon source. S. *cerevisiae*, on the other hand, solely ferments glucose even in the presence of abundant oxygen[6]. A distantly related *Candida* species, *Candida glabrata*, also shuts off respiration in the presence of glucose. As demonstrated in the probe report, toxicity in this fungal species was similarly dependent on growth in glycerol, confirming a requirement for respiration in ML316 toxicity and suggesting a mode of action targeting some aspect of mitochondrial function.

In addition to effectively inhibiting wild-type *Candida* growth, ML316 exhibited potent antifungal activity against the moderately-azole-resistant *C. albicans* strain CaCi-2 (ref. 7) as a single agent (MIC 0.05 μg/ml; **Fig. 1c**). Despite its clinically acquired azole resistance, when CaCi-2 was simultaneously exposed to ML316

[1]Whitehead Institute for Biomedical Research, Cambridge, Massachusetts, USA. [2]Howard Hughes Medical Institute, Department of Biology, Massachusetts Institute of Technology, Cambridge, Massachusetts, USA. [3]Microbiology Graduate Program, Massachusetts Institute of Technology, Cambridge, Massachusetts, USA. [4]Division of Infectious Diseases, Los Angeles Biomedical Research Institute at Harbor-UCLA Medical Center, Torrance, California, USA. [5]Koch Institute for Integrative Cancer Research at Massachusetts Institute of Technology, Cambridge, Massachusetts, USA. [6]Chemical Biology Platform and Probe Development Center, Broad Institute of MIT and Harvard, Cambridge, Massachusetts, USA. [7]David Geffen School of Medicine at UCLA, Los Angeles, California, USA. [8]Present addresses: Benjamin M. Vincent, Yumanity Therapeutics Cambridge, Massachusetts, USA (B.M.V.); Ronin Institute, Montclair, N.J., USA (A.K.L.); Center for Developmental Therapeutics, Broad Institute, Cambridge, Massachusetts, USA (C.L.H.); Ra Pharmaceuticals, Cambridge, Massachusetts, USA (W.Y.) Department of Molecular Genetics,University of Toronto, Toronto, Ontario, Canada (L.W.). [9]Deceased. [10]These authors contributed equally to this work. *e-mail: luke.whitesell@utoronto.ca

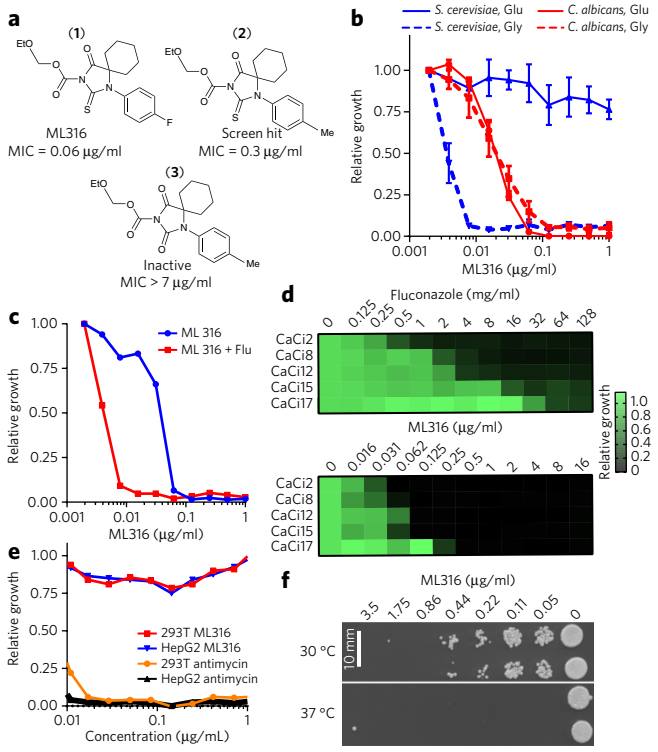

Figure 1 | ML316 is a potent, highly selective fungicide. (**a**) Structures of ML316, the original screen hit and the inactive analog. Minimal inhibitory concentrations (MICs) are indicated for the *C. albicans* strain CaCi-2. Conversion factor for ML316, 1 µM = 0.35 µg/ml. (**b**) Glucose-grown *S. cerevisiae* are not sensitive to ML316. Standard antifungal susceptibility testing was performed in YNB-CSM media with either glucose (Glu, 2% w/v) or glycerol (Gly, 2% w/v) as the carbon source. Optical densities were measured after 24 h at 30 °C and standardized to drug-free controls. The mean of three independent wells is shown. Error bars represent s.e.m. (**c**) ML316 reduces growth of fluconazole-resistant *C. albicans* (strain CaCi-2), an effect that is increased by addition of fluconazole (Flu). Assays in the presence or absence of Flu (8 µg/ml) were performed as in **b** except growth medium consisted of RPMI 1640 with 2% glucose. The mean of two independent wells is shown. (**d**) ML316 inhibits growth of increasingly azole-resistant *C. albicans* strains isolated from the same HIV-infected patient over a 2-year interval. Strain designations are indicated to the left of the heat maps. Sensitivity testing was performed as in **c**. The mean of results from two independent experiments is depicted. (**e**) ML316 is not cytotoxic to human cell lines under respiratory conditions. Viability was assessed by standard resazurin dye-reduction assay after 72 h growth at 37 °C in DMEM supplemented with galactose (10 mM) and dialyzed FBS (10%). Data points depict the mean of measurements from two independent wells for each condition tested. (**f**) ML316 is fungicidal. A standard growth assay was performed as in **c** at either 30 or 37 °C. After 24 h, aliquots were spotted onto YPD agar plates and cultured for an additional 2 d. Scale bar, 10 mm. Data in **c**, **e**, and **f** are derived from one representative experiment. Two independent experiments yielding similar results were performed.

and a threshold concentration of fluconazole, its potency increased greatly (**Fig. 1c**). To better characterize the antifungal activity of the combination, we performed standard checkerboard analysis[8]. Interaction of the compounds was found to be neither formally synergistic nor antagonistic in this strain (**Supplementary Results**, **Supplementary Fig. 1**).

The activity of ML316 against CaCi-2 prompted us to investigate its effects against a wider range of fluconazole-resistant *Candida* strains (**Fig. 1d**). For these experiments, a series of clinical isolates cultured from a single HIV-infected patient over a 2-year period was assessed[7,9]. ML316 remained very active (MIC 0.5 µg/ml) as a single agent against all the isolates tested, including the most fluconazole-resistant strain in the series, CaCi-17 (fluconazole MIC >128 µg/ml). ML316 retained activity against this strain despite the fact that a major contributor to the high-level azole-resistance of CaCi-17 is upregulation of both the ATP-binding cassette (ABC) and multidrug resistance (MDR) efflux pump systems[7], which confer pleiotropic resistance to many small molecules by limiting their intracellular accumulation. To confirm that activity was not limited to one patient series, we tested other azole-resistant strains[10] and found that they also remained sensitive to ML316 (**Supplementary Table 1**). Four strains of the emerging pathogen *Candida auris*, a cause of increasing alarm because of its frequent resistance to known antifungals and potential for epidemic spread in hospital settings, were also tested[11], and were all found to be sensitive to ML316 as well (**Supplementary Table 1**).

Because respiration was required for toxicity in fungi, we evaluated the selectivity of ML316 using human cells grown under conditions enforcing respiration. As expected, a classical inhibitor of respiration, antimycin A, was highly toxic to both 293T (kidney-derived) and HepG2 (liver-derived) cells[12]. Under these same conditions, however, ML316 had no effect on the growth and survival of these cells (**Fig. 1e**). To rule out potential effects of serum on the bioavailability or stability of ML316, experiments were repeated under serum-free growth conditions in which ML316 remained nontoxic to respiring human cells (**Supplementary Fig. 2**).

Many widely used antifungals are cytostatic, stopping the growth of yeast but not killing them. To characterize the nature of ML316's antifungal effects, we performed clonogenic survival assays using the CaCi-2 strain and a broad range of ML316 concentrations (**Fig. 1f**). Fungicidal amphotericin and fungistatic fluconazole served as controls (**Supplementary Fig. 3**). At 24 h, all compounds inhibited growth as measured by the optical density at 600 nm (OD_{600}). Subsequent plating and regrowth in the absence of compound, however, demonstrated that yeast survived at all concentrations of fluconazole tested. In contrast, ML316 and amphotericin were cytocidal at concentrations greater than 1.25 µM at 30 °C. When the incubation temperature was increased to human host range (37 °C), ML316 sensitivity was increased by approximately ten-fold. Such potent, environmentally sensitive fungicidal activity of ML316 led us to move beyond phenotypic characterization and pursue the compound's mode of action and proximal target at the molecular level.

Mitochondrial phosphate carrier mutation confers resistance

We began investigating the molecular basis of ML316 action by selecting for suppressor mutants in *Candida* that could grow in the presence of ML316 (5 µM) under conditions requiring respiration (glycerol as sole carbon source). Mutants emerged at a low rate (~1 in 50 million cells). Genome sequencing of three ML316-resistant mutants from independent selections revealed that they all carried an identical heterozygous mutation (causing the amino acid substitution N184T) in one allele of the *MIR1* gene, which encodes the major mitochondrial P_iC (**Supplementary Fig. 4a**). The Mir1 protein is localized to the inner membrane of mitochondria and carries phosphate into the matrix. No selective small-molecule inhibitors of this protein have been identified. Only low-affinity, nonselective, thiol-reactive agents (such as mersalyl and *N*-ethylmaleimide) have been used to probe its biochemical activity. In genetic experiments, Mir1 is required for respiration in *S. cerevisiae*, but not for its fermentative growth. Requirements for Mir1 have not been studied in *C. albicans* or other fungal pathogens[13–17]. When aligned with its homologs in other species, the asparagine at position 184 of the Mir1 expressed in *Saccharomyces* and *Candida* species was found to be replaced by

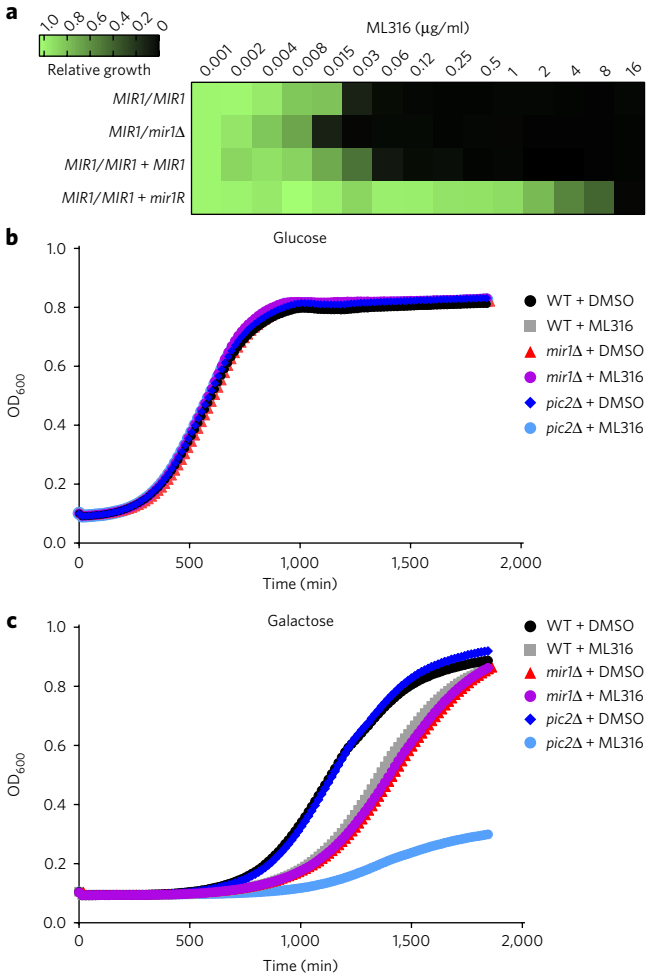

Figure 2 | Genetic evidence for Mir1 as primary target of ML316. (**a**) ML316 sensitivity is correlated with *MIR1* gene dosage and mutation status. Antifungal susceptibility testing with ML316 was performed using wild-type and genetically modified *C. albicans* strains. Relative growth as monitored by OD_{600} was normalized to untreated control for each strain and is displayed in heat map format. Data represent the mean of two independent experiments. (**b**,**c**) ML316 treatment phenocopies the deletion of *MIR1* in *S. cerevisiae*. Change in optical density over time as a measure of growth was monitored in liquid cultures of wild-type (WT) *S. cerevisiae* and the indicated mutant strains. Assays were performed in (**b**) glucose- or (**c**) galactose-supplemented synthetic media with vehicle (DMSO) or ML316 (500 nM) added as indicated. Results are from one of two independent experiments. The mean of measurements from four independent wells is depicted.

threonine, the very same N184T resistance-conferring alteration we found in our suppressor selection experiments. All organisms sensitive to ML316 tested so far have asparagine at this position, whereas all species found to be resistant have threonine, including the human mitochondrial P_iC *SLC25A3* (**Supplementary Fig. 4b**).

Genetic confirmation of Mir1 as target of ML316

To provide further genetic support for Mir1 as the proximal protein target responsible for ML316 action, we constructed *C. albicans* strains that differed in *MIR1* copy number or mutation status. Deletion of one copy of the *MIR1* gene in this diploid organism caused a two-fold decrease in the MIC for ML316, supporting it as the target of this compound on the principle of induced haplo-insufficiency[18]. Integration of an additional wild-type copy of the *MIR1* gene into the genome resulted in an approximately two-fold decrease in sensitivity to ML316. When a mutant copy of *MIR1* encoding the suppressor found in our screen (*mir1R*) was introduced, resistance to ML316 increased 512-fold (**Fig. 2a**). Manipulation of gene copy number and introduction of the suppressor mutant in *S. cerevisiae* grown in glycerol-containing medium produced changes in ML316 sensitivity similar to those demonstrated in *Candida* (**Supplementary Fig. 4c**).

Two functionally redundant mitochondrial P_iCs, Mir1 and Pic2, have been described in *S. cerevisiae*. *C. albicans* also contains a *PIC2* ortholog, C2_09590C. In *S. cerevisiae*, the sequence of Pic2 is 40% identical to that of Mir1, and it has the single amino acid change (N184T) encoded by *mir1R*[19]. *S. cerevisiae* strains were constructed with complete deletion of either *MIR1* or *PIC2* to determine whether ML316 inhibition is specific to Mir1. All strains grew identically in glucose-containing medium supplemented with either vehicle (DMSO) or ML316 (500 nM) (**Fig. 2b**). Strains containing a deletion of *MIR1* cannot grow in glycerol medium, which enforces respiration. In galactose, which can be fermented but requires both respiration and glycolytic fermentation for optimal growth, addition of ML316 decreased the growth of wild-type yeast (**Fig. 2c**). Reduction in growth phenocopied the decrease seen with deletion of *MIR1*, suggesting Mir1 as the target responsible for ML316-induced growth inhibition. ML316-treated *Δmir1* yeast grew similarly to *Δmir1* treated with vehicle, further supporting this conclusion. Growth of our *Δpic2* strain in galactose was identical to that of wild-type yeast. In the presence of ML316, however, growth reduction was even greater than in a *PIC2* wild-type background. We conclude that *S. cerevisiae* Pic2 is insensitive to ML316 and can partially compensate for loss of Mir1 function during growth in galactose.

Functional confirmation of Mir1 as target of ML316

We used a classical assay of mitochondrial phosphate import—the swelling of isolated mitochondria upon incubation in hypertonic ammonium phosphate—to examine the effect of ML316 on uptake of inorganic phosphate into fungal mitochondria (**Fig. 3a**). In this assay, the OD of isolated mitochondria preparations was monitored as a measure of organelle integrity. Freshly prepared mitochondria were suspended in varying hypertonic ammonium salt solutions. Mitochondria are freely permeable to ammonium cation; if its corresponding anion can also enter the mitochondria, they swell and burst, resulting in a rapid decrease in OD of the resultant suspension[16]. As anticipated, incubation of mitochondria in ammonium phosphate buffer resulted in a rapid decline in OD (**Fig. 3a**, upper left panel; blue trace). Phosphate, however, is known to require a carrier function provided by Mir1 to access the matrix and burst mitochondria[16]. Strongly supporting its ability to directly impair Mir1 function, ML316 prevented the decline in OD induced by phosphate (**Fig. 3a**, upper left panel; purple trace). The Mir1 dependence of this effect was confirmed by testing mitochondria isolated from a strain expressing the ML316-resistant N184T mutant encoded by *mir1R*. Phosphate-induced declines in OD were not prevented by ML316 in this background (**Fig. 3a**, upper right panel). As further specificity controls, we tested effects of ML316 on permeability to other anions. We found that loss of mitochondrial integrity caused by acetate, which enters rapidly in a Mir1-independent manner, was not inhibited by ML316 in either genetic background, and integrity in chloride, which is unable to enter intact mitochondria, was likewise unaffected by ML316 (**Fig. 3a**, lower panels).

Role of respiration in ML316-induced toxicity

To directly measure the effect of ML316 on respiration in whole cells, we measured oxygen consumption in *C. albicans* following 10 min of treatment with ML316 (10 μM) or DMSO (**Fig. 3b**, lower panel). Antimycin was then added to determine the nonmitochondrial oxygen consumption rate, which was subtracted from the initial rate to

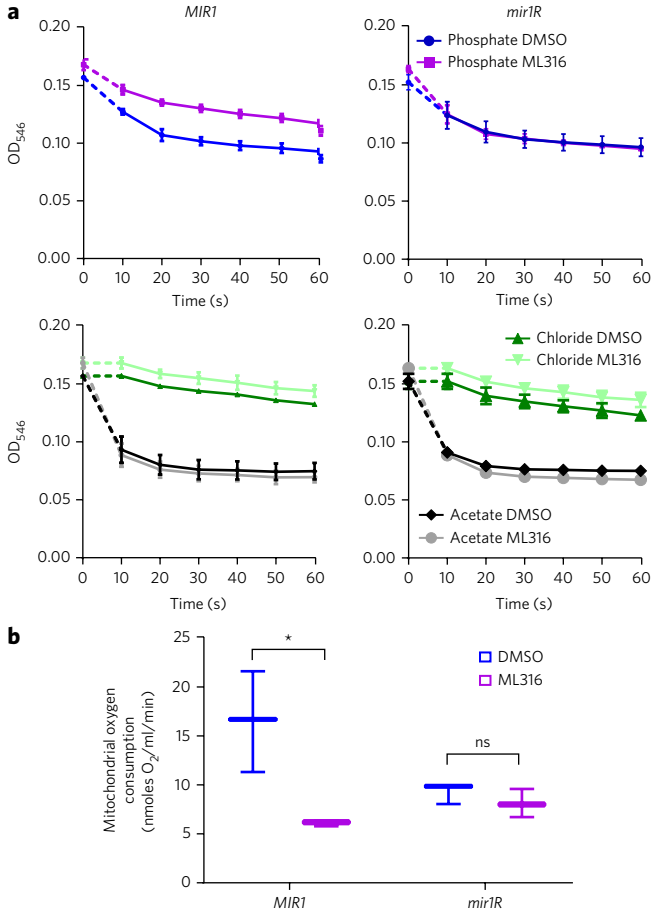

Figure 3 | Biochemical confirmation of ML316 as an inhibitor of Mir1. (**a**) ML316 inhibits phosphate-induced swelling and disruption of purified *C. albicans* mitochondria. The integrity of purified mitochondria isolated from strains expressing an additional copy of either the wild-type (*MIR1*) or drug-resistant *(mir1)* gene version was monitored by optical density (OD). The effect of various inorganic anions on mitochondrial integrity in the presence or absence of ML316 (5 μM) is presented. Relevant buffered salt solution prior to addition of mitochondria served as baseline. Initial measurements were acquired approximately 10 s after addition of mitochondria to each reaction. Three independent aliquots of mitochondria were assayed for each condition, and the entire experiment was performed twice. The mean and s.d. of measurements from one of these experiments is shown. (**b**) ML316 reduces the mitochondrial oxygen consumption (MOC) of *C. albicans* expressing an additional copy of *MIR1*, but not *mir1R*. The MOC rate of *C. albicans* strains grown in glycerol was measured 10 min after addition of ML316 (10 μM) or vehicle control (DMSO). Three independent aliquots of mitochondria were assayed in each of two independent experiments; the mean of one is shown. Error bars, s.e.m. *$P < 0.025$ compared to the DMSO-treated control (unpaired, two-tailed parametric *t*-test).

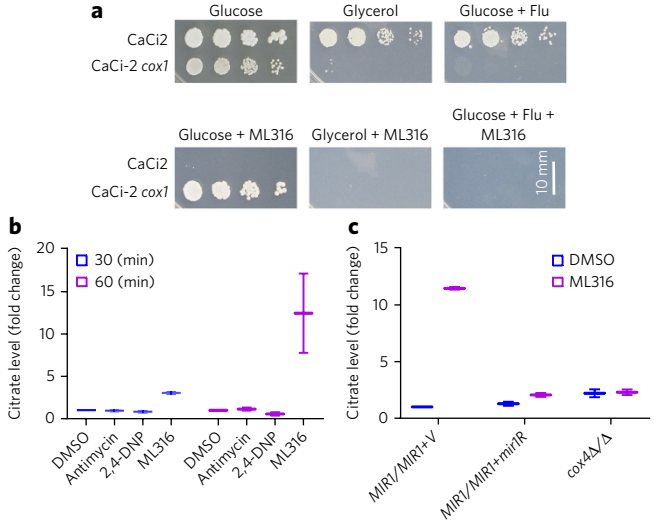

Figure 4 | ML316 renders respiration toxic and increases citrate levels. (**a**) *C. albicans* strain CaCi2 with genetic deletion of mitochondrial *COX1* are resistant to ML316 but are unable to respire or grow in the presence of fluconazole. Serial dilutions of CaCi-2 or CaCi-2 *cox1* were spotted on media with carbon sources supporting fermentation (glucose) or enforcing respiration (glycerol) in presence or absence of ML316 (5 μM) or Flu (16 μM) as indicated. Plates were imaged after 2 d at 30 °C. Scale bar, 10 mm. (**b**) Citrate levels increase dramatically upon treatment with ML316, but not with other mitochondrial poisons. LC–MS was used to measure levels of citrate in *C. albicans* grown in synthetic defined media (2% glucose) following 30 or 60 min exposure to ML316 (5 μM), antimycin (1 μM), or 2,4-dinitrophenol (2,4-DNP; 25 μg/ml). All values were normalized to the mean for DMSO-treated samples. Values represent the mean and s.e.m. from two independent experiments, each consisting of three independent cultures. (**c**) ML316 increases citrate levels in wild-type *Candida*, but not in ML316-resistant mutant strains either expressing *mir1R* or carrying a deletion of *COX4*. Citrate levels were determined by LC–MS in strains growing in glucose after 60 min exposure to ML316 (5 μM). In the genotypes indicated on the *x*-axis, "V" denotes empty vector control. Citrate levels were normalized to the mean of wild type, DMSO-treated samples. Mean and s.e.m. from two independent experiments each consisting of three independent cultures are shown.

yield mitochondrial oxygen consumption (MOC) rate. Our strain with one extra copy of *MIR1* showed a significant decrease in MOC upon ML316 treatment. The strain supplemented with a mutant drug-resistant allele (*mir1R*) displayed a lower, but not statistically significant, decrease (*MIR1*/DMSO versus *mir1R*/DMSO) in basal MOC. Importantly, this MOC did not change significantly with ML316 treatment. These results confirm that inhibition of Mir1 by ML316 impairs mitochondrial respiration. They also suggest that the drug-resistant mutant does not function as well as the wild-type isoform in *Candida* under conditions that require respiration.

To better understand why ML316 was toxic to *C. albicans* even when grown on fermentable carbon sources, we selected for resistant colonies on medium containing ML316 (5 μM) and 2% glucose. Potential resistance-conferring mutations were identified by whole-genome sequencing. Slow-growing colonies emerged at a relatively high frequency (1 colony per 10^5 yeast plated). Sequencing of one of these colonies revealed deletions in the mitochondrially encoded gene *COX1*. This gene encodes a core enzymatic subunit of cytochrome C oxidase (complex IV of the electron transport chain in yeast)[20]. Its activity is required for cellular respiration and growth on nonfermentable carbon sources as demonstrated by the inability of the *cox1* mutant to grow on glycerol-containing media (**Fig. 4a**). This finding indicates that interruption of the electron transport upstream of ATP synthase can rescue the lethality of depleting mitochondrial phosphate with ML316. Ongoing respiration, even when growing in glucose, appears to sensitize *Candida* to ML316. To determine whether this effect was restricted to the *COX1* gene, we evaluated *cox4Δ/Δ* (nuclearly encoded complex IV member) and *rip1Δ/Δ* (nuclearly encoded complex III member) deletion mutants. As a chemical biological complement, we also tested INZ-5, a recently described selective inhibitor of the bc1 complex (**Supplementary Fig. 5**)[2]. All these interventions, which interrupt

electron transport, conferred resistance to ML316. Importantly, the ML316-resistant *cox1* mutant was extremely sensitive to fluconazole even when selected in a strain background with established fluconazole resistance (**Fig. 4a**). This finding is consistent with a previously reported requirement for mitochondrial respiration in azole tolerance[2,21]. Moreover, respiration-defective mutants grow slowly and exhibit reduced virulence[2]. Although resistance to ML316 was achieved under high-glucose conditions *in vitro* by eliminating oxidative phosphorylation, this resistance strategy is unlikely to pose a problem *in vivo*, where the niches occupied by fungi are poor in fermentable substrates and co-administration of azole would greatly disfavor it.

A marked increase in citrate accompanies ML316 toxicity

To better understand the metabolic effects of ML316 in fungi, we compared compound-treated and control-treated yeast by LC–MS-based global polar metabolite profiling. Extracts were prepared from *C. albicans* growing in glucose that had been treated for 90 min with ML316 with electron transport chain poisons (rotenone, antimycin, and potassium cyanide), or with the uncouplers 2,4-dinitrophenol(2,4-DNP)andcarbonylcyanide-4-(trifluoromethoxy) phenylhydrazone (FCCP). As expected, blocking electron transport altered the levels of a wide range of polar metabolites. Succinate and citrate showed the largest changes, reaching a threshold of greater than four-fold ($\log_2$ change > 2; **Supplementary Table 2**). Succinate levels decreased 4.25 ± 0.6-fold in two independent experiments. A decrease in succinate appeared to be common in all the compounds tested, with FCCP driving the greatest alteration (5.5 ± 1-fold reduction). Unique to ML316, however, we found a dramatic (>7-fold) increase in levels of citrate, a central player in mitochondrial metabolism (**Fig. 4b**). Electron transport chain inhibitors caused only a mild (<2-fold) induction in citrate levels, and uncouplers had a minimal effect. In follow-up experiments focused on citrate alterations, levels rose three-fold within 30 min of ML316 treatment and >12-fold at 60 min post-treatment (**Fig. 4b**). In contrast, we observed no major changes in cells treated with the classical mitochondrial poisons antimycin or 2,4-DNP. We also measured citrate levels after ML316 treatment in our resistant mutants. In cells expressing the Mir1 N184T variant or in cells resistant due to loss of cytochrome oxidase activity (*cox4*Δ/Δ), there was no significant increase in citrate levels (**Fig. 4c**). At this point, we have no evidence that citrate accumulation is directly responsible for the fungicidal activity of ML316. Nevertheless, our genetic and biochemical evidence establishes the dependence of this accumulation on depletion of mitochondrial phosphate in the context of ongoing electron transport. As a signature effect, distinct from that of all other mitochondrial poisons tested, citrate accumulation could provide a valuable point of departure in probing the mechanism(s) by which electron transport is coordinated with ATP production in mitochondria.

ML316 inhibits azole-resistant *C. albicans* in mice

Previous characterization of ML316 pharmacokinetics revealed poor plasma stability for the compound, precluding its testing in mouse models of systemic candida infection. To overcome this limitation and investigate its antifungal potential *in vivo*, we evaluated ML316 in a well-accepted mouse model of oropharyngeal candidiasis (OPC)[22,23]. Mucosal candida infections are a common, often debilitating problem in a variety of clinical settings associated with inborn or acquired deficiencies of T-cell-mediated immune function and are often complicated by the emergence of azole resistance.

To test ML316, we pretreated mice with corticosteroids to induce susceptibility and then infected them sublingually with azole-resistant *C. albicans* originally isolated from an HIV patient with recurrent OPC[7]. After allowing the infection to establish for 3 d, cohorts of mice were treated with fluconazole, ML316 or the combination. Fluconazole was administered systemically, whereas ML316 was simply added to the drinking water of animals. Antifungal activity was assessed by measuring residual colony forming units (CFU) persisting on the tongue after completing 2 d of therapy. ML316 treatment decreased fungal burden by approximately 100-fold (**Fig. 5a**). Treatment with fluconazole alone resulted in a similar reduction in fungal burden, while the combination of both fluconazole and ML316 dropped fungal burden by >1,000-fold. Microscopic examination of periodic acid–Schiff (PAS)-stained tissue sections was consistent with CFU quantitation. Fields containing fungi were selected for imaging and presentation to demonstrate the effects

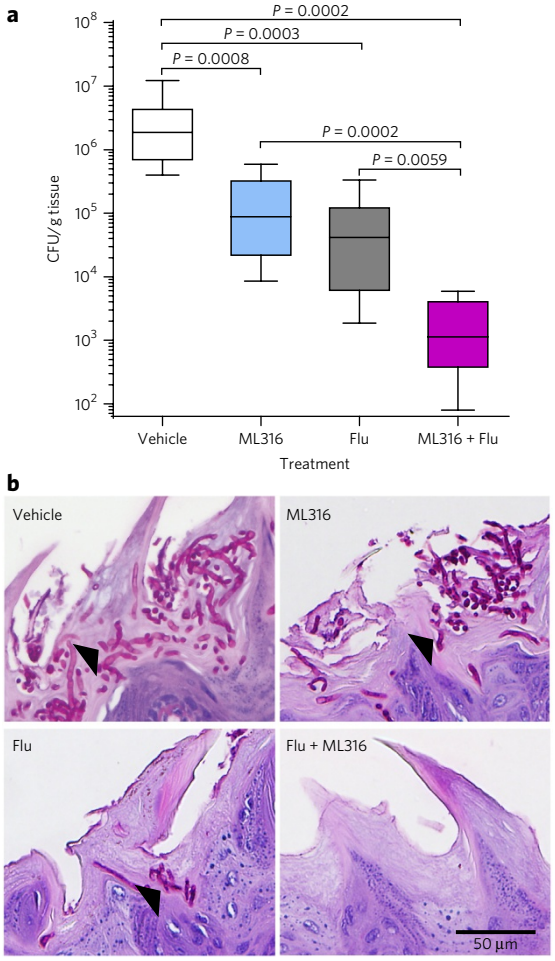

Figure 5 | ML316 is active against azole-resistant *C. albicans* in mice. (**a**) Mice were treated with corticosteroids to induce susceptibility and infected sublingually with strain CaCi-2. Three days later, they were randomly assigned to treatment as indicated (n = 8 mice per group except fluconazole (Flu; n = 7)). ML316 was added to drinking water (2.85 µM ML316/ 1% w/v sucrose and 0.001% v/v PEG400) while Flu was administered intraperitoneally (10 mg/kg/day). Antifungal activity was assessed by measuring residual colony forming units (CFU) persisting on the tongue after completing 2 d of therapy. Center line, median; box limits, 25th to 75th percentile; whiskers, data minimum and maximum. The statistical significance of differences between treatment groups was determined by the Mann-Whitney test (unpaired, two-tailed, nonparametric). *P* values are indicated above the relevant comparisons (Flu vs. ML316; not significant). (**b**) Photomicrographs of PAS-stained tissue sections to assess fungal morphology are presented. Arrowheads indicate fungal foci, which appear dark pink against the lighter staining of the keratinized papillae of the host tongue. Control mice received drinking water supplemented with 1% w/v sucrose and 0.001% PEG400 Scale bar, 50 mm.

on morphology (**Fig. 5b**). Control mice had multiple, superficially destructive lesions; a few small, dystrophic lesions were seen in tissue from mice receiving either fluconazole or ML316. No lesions were identified in mice receiving combination therapy. Equally as important, no histological evidence of toxicity to normal tissues from topical exposure to ML316 was seen. ML316 treatment also appeared to impair the filamentation of the *C. albicans*. The ability of fungi to switch between yeast and filamentous forms is a critical determinant of fungal virulence due to its role in tissue invasion[24]. Overall, results indicate that ML316 is well tolerated topically, has significant antifungal activity alone and that combination with fluconazole *in vivo* provides greater efficacy, even against a *Candida* isolate with pre-existing azole resistance.

DISCUSSION

Pathogenic fungi are remarkably resilient organisms that pose a rapidly increasing threat to human health in large part because of our limited therapeutic arsenal and their ability to cause life-threatening systemic infections in patients with impaired immune function. The most frequently isolated fungal pathogen in humans is the yeast *C. albicans*[25]. This organism is capable of shifting between distinct morphological states and altering its central metabolism to invade diverse niches in humans, form biofilms, and resist available antifungals[26].

Mitochondria have been identified as key players in the adaptive abilities of *C. albicans* and other fungi, enabling virulence, morphogenesis, and drug resistance[21,27,28]. Many molecular details remain to be defined, but efforts to identify novel elements and functional diversity in the electron transport chain of pathogenic fungi have been reported[29]. Here, we identify the compound ML316 as an inhibitor of the mitochondrial P_iC Mir1. Under respiratory conditions, ML316 transforms mitochondria from enablers of drug resistance and pathogenesis to active instigators of fungal cell death. In addition to the value of this reagent as a chemical probe to enable basic studies, our findings demonstrate that converting fungal respiration to a toxic process by impairing phosphate uptake is feasible in animals and could provide a much needed new treatment strategy.

Mitochondrial P_iCs perform a critical function in eukaryotes. Under normal conditions, most of the energy required by cells is supplied by the generation of ATP in their mitochondria. Production takes place in the mitochondrial matrix, where ATP synthase generates ATP from ADP and inorganic phosphate (P_i) using the electromotive force of a proton gradient sustained by the electron transport chain. Flux through this reaction is carefully controlled by the availability of its substrates, ADP and P_i. In the fungus *S. cerevisiae* the P_i carrier Mir1 has been shown to be essential for respiratory growth[13]. Here we have shown that selective chemical inhibition of this P_iC in *C. albicans* is lethal, even in standard high-glucose media, enabling energy generation by fermentation.

Although P_iC proteins are similar in humans and fungi, previous experiments have indicated that P_i itself plays a unique role in the mitochondria of fungi. Mir1 has been identified as part of the fungal mitochondrial unspecific channel (MUC)[30]. In fungi, the presence of phosphate in the inner mitochondrial matrix is essential for preventing uncoupling of electron transport and loss of membrane potential owing to opening of the MUC. This does not appear to be case for mammalian mitochondria. Differences in the stimuli that inhibit and activate the opening of MUCs in plants, fungi, and mammals have been reported, but the physiological relevance of these differences is not yet clear[31]. Although inhibition of P_iC by mersalyl, a nonspecific organomercury compound, was critical for early experiments defining the function of the P_iC[14,15] and the MUC in purified mitochondria[30], no compounds have been previously described that selectively inhibit a P_iC. Discovery of ML316 opens new avenues for research in this area and related aspects of mitochondrial phosphate biology because the compound is cell permeant, highly target selective, and species specific.

The species specificity of ML316 appears to be a result of a single amino acid difference in the fungal protein Mir1 as compared to the homologous human P_iC. Surprisingly, both fungal species we studied have homologs of *MIR1* in their genomes that encode the same single amino acid change present in the resistant allele of humans. Designated as Pic2 in *S. cerevisiae*, overexpression of this second P_iC in a *mir1Δ/pic2Δ* background is reported to rescue the deletion strain's growth defect on nonfermentable carbon sources and restore phosphate uptake into the mitochondrial matrix[19]. Interestingly, although *S. cerevisiae* has ML316-resistant Pic2 encoded in its nuclear genome, its expression imparts only partial protection against ML316 during growth in galactose. Moreover, the organism remains very sensitive to ML316 when respiration is strictly enforced by growth in glycerol. Additionally, we never recovered any mutations involving *PIC2* in our drug-resistance selection experiments.

Although ML316 was active on its own, it was more effective when combined with an azole. Combination therapy remains a much-underutilized approach for the management of fungal infections despite being routine for the treatment of bacterial infections. The phenotypic screening strategy that led to the work with ML316 reported here and previous studies by us and others suggest that a productive strategy to develop useful antifungal combinations will involve combining azoles already in widespread use with new agents targeting mitochondrial function[2].

Additional medicinal chemistry will be required to address the pharmacological liabilities of ML316 and generate a true drug candidate for either topical or systemic applications. The ethyl carbamate of ML316 appears to be the primary source of instability, because replacing the carbamate with a methyl group significantly increases plasma stability. Carbamates can be susceptible to metabolic hydrolysis by numerous esterases, a feature that has been exploited in the design and synthesis of prodrugs[32]. Because the saliva of humans and rodents is rich in esterase activity[33], most of the material we provided to mice in their drinking water was probably degraded rapidly upon intake, resulting in relatively limited mucosal exposure to active compound, especially during the animals' daytime sleep cycle when oral intake drops. Despite these limitations we demonstrated a highly significant effect of ML316 against azole-resistant *C. albicans* in mice, establishing the value of Mir1 as an antifungal target. Based on insights from the limited SAR studies performed during development of ML316 as a probe, embedding its ethyl carbamate into an oxazole or similar ring systems might provide a feasible approach to overcoming its metabolic instability.

ML316 appears to be a poor substrate for the major drug efflux pumps. Late isolates in the *C. albicans* clinical series we studied have marked drug pump overexpression, but remained sensitive to the compound. In culture, we identified two other mechanisms, however, by which resistance to ML316 can be acquired. Mutations that disrupt electron transport arose with relatively high frequency under growth conditions supporting fermentative metabolism. From a therapeutic perspective, these mutants should be irrelevant because they cannot respire. This defect cripples virulence by restricting nutrient utilization and impairing filamentation while concomitantly conferring extreme sensitivity to fluconazole. Another mechanism of acquired resistance, mutation of the *MIR1* target gene itself, occurred with very low frequency and only arose when growth was restricted to a respiratory substrate. The recurring mutation in *MIR1* that we recovered was hypomorphic, imparting a moderate defect in cellular respiration. Therefore, for both modes of acquired resistance identified, the development of resistance carried debilitating fitness costs. In a mammalian host, these mechanisms would greatly impair virulence, strongly disfavoring their emergence. From a broader evolutionary perspective, targeting Mir1 with ML316 is an attractive strategy because it confronts the fungus with conflicting selective pressures. Respiration is needed for survival, virulence, and azole resistance in the host, but ongoing electron transport poisons the cell. Creation of such a dilemma offers

a much needed approach to the development of new, resistance-evasive antifungal treatment regimens.

Received 1 June 2017; accepted 27 October 2017;
published online 11 December 2017

METHODS

Methods, including statements of data availability and any associated accession codes and references, are available in the online version of the paper.

References

1. Cowen, L.E. & Lindquist, S. Hsp90 potentiates the rapid evolution of new traits: drug resistance in diverse fungi. *Science* **309**, 2185–2189 (2005).
2. Vincent, B.M. *et al.* A fungal-selective cytochrome bc1 inhibitor impairs virulence and prevents the evolution of drug resistance. *Cell Chem. Biol.* **23**, 978–991 (2016).
3. Baell, J.B. & Holloway, G.A. New substructure filters for removal of pan assay interference compounds (PAINS) from screening libraries and for their exclusion in bioassays. *J. Med. Chem.* **53**, 2719–2740 (2010).
4. Tran, C. *et al.* Development of a Second-Generation Antiandrogen for Treatment of Advanced Prostate Cancer. *Science* **324**, 787–790 (2009).
5. Hartland, C.L. *et al.* Probing Metabolic Requirements for Fungal Virulence — Probe 1 https://www.ncbi.nlm.nih.gov/books/NBK143544/ (National Center for Biotechnology Information, Bethesda, 2012).
6. Strijbis, K. & Distel, B. Intracellular acetyl unit transport in fungal carbon metabolism. *Eukaryot. Cell* **9**, 1809–1815 (2010).
7. White, T.C. Increased mRNA levels of *ERG16, CDR*, and *MDR1* correlate with increases in azole resistance in Candida albicans isolates from a patient infected with human immunodeficiency virus. *Antimicrob. Agents Chemother.* **41**, 1482–1487 (1997).
8. Orhan, G., Bayram, A., Zer, Y. & Balci, I. Synergy tests by E test and checkerboard methods of antimicrobial combinations against Brucella melitensis. *J. Clin. Microbiol.* **43**, 140–143 (2005).
9. Ford, C.B. *et al.* The evolution of drug resistance in clinical isolates of Candida albicans. *eLife* **4**, e00662 (2015).
10. Perea, S. *et al.* Prevalence of molecular mechanisms of resistance to azole antifungal agents in *Candida albicans* strains displaying high-level fluconazole resistance isolated from human immunodeficiency virus-infected patients. *Antimicrob. Agents Chemother.* **45**, 2676–2684 (2001).
11. Clancy, C.J. & Nguyen, M.H. Emergence of candida auris: An international call to arms. *Clin. Infect. Dis.* **64**, 141–143 (2017).
12. Marroquin, L.D., Hynes, J., Dykens, J.A., Jamieson, J.D. & Will, Y. Circumventing the Crabtree effect: replacing media glucose with galactose increases susceptibility of HepG2 cells to mitochondrial toxicants. *Toxicol. Sci.* **97**, 539–547 (2007).
13. Murakami, H., Blobel, G. & Pain, D. Isolation and characterization of the gene for a yeast mitochondrial import receptor. *Nature* **347**, 488–491 (1990).
14. Tyler, D.D. Evidence of a phosphate-transporter system in the inner membrane of isolated mitochondria. *Biochem. J.* **111**, 665–678 (1969).
15. Phelps, A., Schobert, C.T. & Wohlrab, H. Cloning and characterization of the mitochondrial phosphate transport protein gene from the yeast *Saccharomyces cerevisiae*. *Biochemistry* **30**, 248–252 (1991).
16. Zara, V. *et al.* Yeast mitochondria lacking the phosphate carrier/p32 are blocked in phosphate transport but can import preproteins after regeneration of a membrane potential. *Mol. Cell. Biol.* **16**, 6524–6531 (1996).
17. Seifert, E.L., Ligeti, E., Mayr, J.A., Sondheimer, N. & Hajnóczky, G. The mitochondrial phosphate carrier: role in oxidative metabolism, calcium handling and mitochondrial disease. *Biochem. Biophys. Res. Commun.* **464**, 369–375 (2015).
18. Giaever, G. *et al.* Genomic profiling of drug sensitivities via induced haploinsufficiency. *Nat. Genet.* **21**, 278–283 (1999).
19. Hamel, P. *et al.* Redundancy in the function of mitochondrial phosphate transport in *Saccharomyces cerevisiae* and *Arabidopsis* thaliana. *Mol. Microbiol.* **51**, 307–317 (2004).
20. Lemaire, C., Robineau, S. & Netter, P. Molecular and biochemical analysis of *Saccharomyces cerevisiae* cox1 mutants. *Curr. Genet.* **34**, 138–145 (1998).
21. Sun, N. *et al.* Azole susceptibility and transcriptome profiling in *Candida albicans* mitochondrial electron transport chain complex I mutants. *Antimicrob. Agents Chemother.* **57**, 532–542 (2013).
22. Solis, N.V. & Filler, S.G. Mouse model of oropharyngeal candidiasis. *Nat. Protoc.* **7**, 637–642 (2012).
23. Swidergall, M. & Filler, S.G. Oropharyngeal Candidiasis: fungal invasion and epithelial cell responses. *PLoS Pathog.* **13**, e1006056 (2017).
24. Shapiro, R.S., Robbins, N. & Cowen, L.E. Regulatory circuitry governing fungal development, drug resistance, and disease. *Microbiol. Mol. Biol. Rev.* **75**, 213–267 (2011).
25. Pfaller, M.A. & Diekema, D.J. Epidemiology of invasive candidiasis: a persistent public health problem. *Clin. Microbiol. Rev.* **20**, 133–163 (2007).
26. Noble, S.M., Gianetti, B.A. & Witchley, J.N. *Candida albicans* cell-type switching and functional plasticity in the mammalian host. *Nat. Rev. Microbiol.* **15**, 96–108 (2017).
27. Shingu-Vazquez, M. & Traven, A. Mitochondria and fungal pathogenesis: drug tolerance, virulence, and potential for antifungal therapy. *Eukaryot. Cell* **10**, 1376–1383 (2011).
28. Grahl, N. *et al.* Mitochondrial activity and Cyr1 are key regulators of Ras1 activation of *C. albicans* virulence pathways. *PLoS Pathog.* **11**, e1005133 (2015).
29. Li, D., She, X. & Calderone, R. Functional diversity of complex I subunits in Candida albicans mitochondria. *Curr. Genet.* **62**, 87–95 (2016).
30. Gutiérrez-Aguilar, M., Pérez-Martínez, X., Chávez, E. & Uribe-Carvajal, S. In Saccharomyces cerevisiae, the phosphate carrier is a component of the mitochondrial unselective channel. *Arch. Biochem. Biophys.* **494**, 184–191 (2010).
31. Cortés, P., Castrejón, V., Sampedro, J.G. & Uribe, S. Interactions of arsenate, sulfate and phosphate with yeast mitochondria. *Biochim. Biophys. Acta.* **1456**, 67–76 (2000).
32. Ghosh, A.K. & Brindisi, M. Organic carbamates in drug design and medicinal chemistry. *J. Med. Chem.* **58**, 2895–2940 (2015).
33. Yoshimura, Y., Morishita, M., Mori, M. & Kawakatsu, K. Zymograms and histochemistry of non-specific esterase in the salivary glands. *Histochemie* **18**, 302–313 (1969).

Acknowledgments

Thanks to M.V. Heiden, V. Mootha and R. Mazitschek for helpful discussions. We also thank the Whitehead GTC, especially J. Love, T. Volkert, and S. Gupta for assistance with genome sequencing. We thank E. Freinkman (Whitehead Metabolomics Core) for assistance with metabolite profiling. Susan Lindquist was an HHMI investigator. Additional support was provided by NIH grants R01DE022600 (S.G.F.), U54HG005032-1 (Stuart Schreiber, Broad Institute), R03MH08645601 (S.L.) and R01AI120958-01A1 (L.W.). A postdoctoral fellowship from the American Cancer Society supported L.B.S. while B.M.V. was supported in part by an NSF graduate research fellowship and the Mathers Foundation. We thank T. White (University of Missouri—Kansas City), A. Mitchell (Carnegie Mellon University) and S. Nobel (UCSF) for yeast strains.

Author contributions

L.W., S.L., B.M.V., and C.A.M. conceived and designed the study. C.A.M., B.M.V., and L.W. performed microbiological, genetic, biochemical, and metabolic studies. B.M.V. and A.K.L. analyzed whole fungal genome sequencing data. C.L.H. performed the primary and follow-up screening work that led to the identification of ML316. W.Y. provided chemistry advice and synthesized ML316. L.B.S. performed the oxygen consumption experiments. N.V.S., S.G.F., and L.W. designed, performed, and analyzed animal experiments.

Competing financial interests

The authors declare competing financial interests: details accompany the online version of the paper.

Additional information

Any supplementary information, chemical compound information and source data are available in the online version of the paper. Reprints and permissions information is available online at http://www.nature.com/reprints/index.html. Publisher's note: Springer Nature remains neutral with regard to jurisdictional claims in published maps and institutional affiliations. Correspondence and requests for materials should be addressed to L.W.

ONLINE METHODS

Chemical matter. For a full description of the synthesis and purity of compounds **1**, **2** and **3** (ML316), please refer to the Molecular Libraries probe report[5]. Synthesis of INZ-5 has been previously reported[2]. Fluconazole was obtained from Sequoia Research Products (cat. #SRP01025f) with a purity of >99%. Antimycin A was purchased from Sigma (cat. #A8674) as a mixture of antimycins that conforms to specifications. 2,4 DNP was purchased from Sigma (D198501), purity >98%. Amphotericin B was purchased from Sigma (A2411), purity ~80% (suitable for tissue culture). Rotenone was also from Sigma (R8875), purity 95–98%.

Yeast strains and human cell lines. The fluconazole-resistant *C. albicans* series CaCi-2,CaCi-8, CaCi-12, CaCi-15 and CaCi-17 was obtained from Ted White[7]. Other resistant *C. albicans* pairs were provided by A. Mitchell[34]. Deletions mutants *Δrip1/Δrip1* and *Δcox4/Δcox4* were a gift from S. Nobel[35]. **Supplementary Table 1** contains the source information for other strains included therein. The human cell lines HepG2 and 293T were purchased from the American Type Culture collection (ATCC) and confirmed negative for mycoplasma contamination by PCR-based testing.

Antifungal susceptibility testing. The antiproliferative activity of compounds in media supplemented with glucose, galactose or glycerol was measured using standard antifungal susceptibility protocols[36]. After 24 h the optical density at 600 nm (OD_{600}) was read in 96-well format using an Envision plate reader. To assess the fungicidal activity of compounds, cultures growing in 96-well liquid format, were resuspended with a multichannel pipette and spotted to fresh, drug-free yeast extract peptone dextrose (YPD) plate using a metal frogger. Plates were then incubated at 30 °C for an additional 2 d before image capture. Checkerboard analysis was performed as previously described[8].

Suppressor mutant isolation and identification. *C. albicans* strains SC5314 or CaCi-2 were grown to saturation overnight in Difco Yeast-Nitrogen-Base with complete amino acid supplementation (YNB-CSM) with 2% glucose, pelleted by centrifugation, and resuspended in phosphate-buffered saline. Approximately 10^7 cells were plated onto agar medium formulated with ML316 (5 μM) in YNB-CSM and either 2% glucose or 2% glycerol as the carbon source. After 5 d, colonies that emerged were restreaked on the same media to isolate single colonies. These colonies were expanded in liquid culture for preparation of genomic DNA using a Yeastar genomic DNA extraction kit (Zymo Research). Genome sequencing and bio-informatic analysis was performed as described previously[37].

Metabolite profiling. An overnight culture of *C. albicans* was diluted into YNB-CSM-2% glucose media at an OD_{600} of 0.25, grown for 3 h to mid-log phase, and then split into parallel 5-ml cultures for treatment with compounds (DMSO, 20 μM rotenone, 1 μM antimycin, 5 mM potassium cyanide, 20 μM oligomycin, 25 μg/ml 2,4-dinitrophenol, 32 μM FCCP, 2.5 μM ML316). After growth with compounds for the indicated time intervals, cultures were pelleted, washed once in PBS, and frozen in liquid nitrogen. Polar metabolites were extracted by resuspending cells in 600 μl methanol, 300 μl water, and 400 μl chloroform, and adding 100 μl of glass beads before vortexing for 60 s. Samples were then centrifuged for 10 min at 13,000*g*, and the supernatant (polar) layer was moved to a new microcentrifuge tube, and evaporated by Speedvac. Samples were then subjected to LC–MS/MS profiling on a Thermo Orbitrap platform, as described previously[38].

Phosphate swelling assays. *C. albicans* strains were grown in yeast extract-peptone-glycerol (3% w/v) media (YPG) at 30 °C with shaking. Intact mitochondria were isolated using a standard procedure for *S. cerevisiae* as previously published[39]. The phosphate swelling assays were performed as described[16] with the several modifications. To assess turbidity changes induced by addition of specific anions in the presence of test compounds, the cassette attachment of a Multiskan Go instrument was used (Thermo Fisher). The instrument was programmed for a kinetic run at 30 °C, monitoring OD_{544} and reading every 10 s. To start the experiment 40 μl of mitochondria (100 μg total protein) was added to 1 ml of salt solution in a disposable cuvette, vortexed and the run started. Prior to reading, 10 μM ML316 or an equivalent amount of DMSO was added to 100 μg of mitochondria on ice. Three replicates were run for each condition and the experiment repeated in full once.

Mitochondrial oxygen consumption. *C. albicans* strains were pregrown in 3% glycerol YNB-CSM media at 30 °C. The oxygen consumption of exponentially growing cells was measured at 30 °C with an Oxytherm oxygraph (Hansatech Instruments, Norfolk, England). Four OD_{600} units of cells were resuspended in 2 ml of growth media and then split into two aliquots. Ten minutes before measurement, 10 μM ML316 was added to one aliquot and an equivalent volume of vehicle (1 μl DMSO) to the other aliquot. Mitochondrial oxygen consumption (MOC) rate was allowed to stabilize for a short interval then measured over three equal time periods and averaged. 50 μM antimycin was then added, and the rate was measured again over three time windows and averaged. The average antimycin-treated rate was subtracted from the nonantimycin rate for each experimental condition tested to calculate MOC rate.

Oropharyngeal candidiasis model. Female, 4–6-week-old BALB/c mice were immunosuppressed with cortisone acetate as previously described[22]. Animals were subsequently inoculated sublingually with *C. albicans* strain CaCi-2. To do so, animals were sedated with ketamine and xylazine, after which calcium alginate swabs that had been soaked in Hanks' balanced salt solution containing 10^6 *C. albicans* cells/ml were placed sublingually for 90 min. After 3 d to allow establishment of infection, cages of mice were randomly assigned to experimental groups and treatment with antifungal compounds begun. No blinding was performed. Cohort size was determined based on prior experience with this animal model. ML316 (3.2 μM) was administered *ad lib* in drinking water supplemented with sucrose (1% w/v) to increase palatability. To aid in formulation, a concentrated stock solution of ML316 was prepared at 1 mg/ml in PEG 400, stored at −20 °C until use and diluted into fresh sucrose-containing water daily. Control mice received sucrose-containing drinking water supplemented with an equal volume of PEG 400 vehicle (0.001% v/v). Fluconazole was administered intraperitoneally at 10 mg/kg/d. Mice were euthanized 5 d after fungal infection, and the tongues were divided longitudinally. One half was weighed and homogenized in PBS for quantitative culture. The other half was fixed in zinc-buffered formalin and embedded in paraffin, after which thin sections were cut and stained with Periodic acid–Schiff (PAS). All treatment groups consisted of eight animals except the fluconazole group, which had seven animals. All animal experimentation was performed under a protocol approved by the Institutional Animal Care and Use Committee (IACUC) of the Los Angeles Biomedical Research Institute.

Statistics. GraphPad Prism 7 was used to generate all statistics reported. Replicate numbers (*n* values) are provided in the relevant figure legends. The *t*-tests reported in **Figure 3b** are unpaired, two-tailed, parametric values. The exact *P* values for the comparisons shown are *MIR1* DMSO versus *MIR1* ML316, $P = 0.0248$; *MIR1* DMSO versus *mir1R* DMSO, $P = 0.0751$; and *mir1R* DMSO versus *mir1R* ML316, $P = 0.3227$. The Mann–Whitney tests reported in **Figure 5** are two tailed, unpaired, nonparametric calculations. The exact *P* value for comparison of ML316 and fluconazole reported as not significant is $P = 0.2949$. All other *P* values are indicated in the figure.

Life Sciences Reporting Summary. Further information on experimental design and reagents is available in the **Life Sciences Reporting Summary**.

Data Availability. Genomic sequence data presented in this study are available for download from NCBI bioproject at http://www.ncbi.nlm.nih.gov/bioproject/388652 (Bioproject accession number PRJNA388652), and at the NCBI SRA at http://www.ncbi.nlm.nih.gov/Traces/study/?acc=SRP108351 (accession number SRP108351)

34. Bruno, V.M. & Mitchell, A.P. Regulation of azole drug susceptibility by *Candida albicans* protein kinase CK2. *Mol. Microbiol.* **56**, 559–573 (2005).
35. Noble, S.M., French, S., Kohn, L.A., Chen, V. & Johnson, A.D. Systematic screens of a *Candida albicans* homozygous deletion library decouple morphogenetic switching and pathogenicity. *Nat. Genet.* **42**, 590–598 (2010).

doi:10.1038/nchembio.2534

36. Xie, J.L., Singh-Babak, S.D. & Cowen, L.E. Minimum inhibitory concentration (MIC) assay for antifungal drugs. *Bio Protoc.* **2**, e252 (2012).
37. Vincent, B.M., Lancaster, A.K., Scherz-Shouval, R., Whitesell, L. & Lindquist, S. Fitness trade-offs restrict the evolution of resistance to amphotericin B. *PLoS Biol.* **11**, e1001692 (2013).
38. Birsoy, K. *et al.* An essential role of the mitochondrial electron transport chain in cell Proliferation is to enable aspartate synthesis. *Cell* **162**, 540–551 (2015).
39. Morizono, H., Woolston, J.E., Colombini, M. & Tuchman, M. The use of yeast mitochondria to study the properties of wild-type and mutant human mitochondrial ornithine transporter. *Mol. Genet. Metab.* **86**, 431–440 (2005).

nature research

Corresponding author(s): Luke Whitesell

☐ Initial submission ☐ Revised version ☒ Final submission

Life Sciences Reporting Summary

Nature Research wishes to improve the reproducibility of the work that we publish. This form is intended for publication with all accepted life science papers and provides structure for consistency and transparency in reporting. Every life science submission will use this form; some list items might not apply to an individual manuscript, but all fields must be completed for clarity.

For further information on the points included in this form, see Reporting Life Sciences Research. For further information on Nature Research policies, including our data availability policy, see Authors & Referees and the Editorial Policy Checklist.

Experimental design

1. Sample size

Describe how sample size was determined.

For all microbiological and cell culture experiments, the number of biological replicates performed was chosen on the basis of experimental feasibility and previously established operating procedures in the lab for the specific assay performed

2. Data exclusions

Describe any data exclusions.

No data were excluded

3. Replication

Describe whether the experimental findings were reliably reproduced.

All attempts at replication were successful.

4. Randomization

Describe how samples/organisms/participants were allocated into experimental groups.

No specific method was used to randomize the allocation of mice to experimental groups. Allocation of the animals into groups is described in the manuscript p33.

5. Blinding

Describe whether the investigators were blinded to group allocation during data collection and/or analysis.

No blinding was performed as stated in the manuscript p33.

Note: all studies involving animals and/or human research participants must disclose whether blinding and randomization were used.

6. Statistical parameters

For all figures and tables that use statistical methods, confirm that the following items are present in relevant figure legends (or in the Methods section if additional space is needed).

n/a	Confirmed	
☐	☒	The exact sample size (*n*) for each experimental group/condition, given as a discrete number and unit of measurement (animals, litters, cultures, etc.)
☐	☒	A description of how samples were collected, noting whether measurements were taken from distinct samples or whether the same sample was measured repeatedly
☐	☒	A statement indicating how many times each experiment was replicated
☐	☒	The statistical test(s) used and whether they are one- or two-sided (note: only common tests should be described solely by name; more complex techniques should be described in the Methods section)
☐	☒	A description of any assumptions or corrections, such as an adjustment for multiple comparisons
☐	☒	The test results (e.g. *P* values) given as exact values whenever possible and with confidence intervals noted
☐	☒	A clear description of statistics including central tendency (e.g. median, mean) and variation (e.g. standard deviation, interquartile range)
☐	☒	Clearly defined error bars

See the web collection on statistics for biologists for further resources and guidance.

Nature Chemical Biology: doi:10.1038/nchembio.2534

Software

Policy information about availability of computer code

7. Software

Describe the software used to analyze the data in this study.	Data was analyzed using Prism.

For manuscripts utilizing custom algorithms or software that are central to the paper but not yet described in the published literature, software must be made available to editors and reviewers upon request. We strongly encourage code deposition in a community repository (e.g. GitHub). *Nature Methods* guidance for providing algorithms and software for publication provides further information on this topic.

Materials and reagents

Policy information about availability of materials

8. Materials availability

Indicate whether there are restrictions on availability of unique materials or if these materials are only available for distribution by a for-profit company.	Compounds described are only available from us in limited quantities.

9. Antibodies

Describe the antibodies used and how they were validated for use in the system under study (i.e. assay and species).	No antibodies were used.

10. Eukaryotic cell lines

a. State the source of each eukaryotic cell line used.	Cell lines were purchased from the ATCC
b. Describe the method of cell line authentication used.	The cell lines were not authenticated for the purposes of this study because their specific identity is non-critical to the conclusions drawn
c. Report whether the cell lines were tested for mycoplasma contamination.	The cell lines were tested for mycoplasma contamination.
d. If any of the cell lines used are listed in the database of commonly misidentified cell lines maintained by ICLAC, provide a scientific rationale for their use.	Cell lines are not listed in the database.

Animals and human research participants

Policy information about studies involving animals; when reporting animal research, follow the ARRIVE guidelines

11. Description of research animals

Provide details on animals and/or animal-derived materials used in the study.	Female, 4-6 week old BALB/c mice were used.

Policy information about studies involving human research participants

12. Description of human research participants

Describe the covariate-relevant population characteristics of the human research participants.	No human research participants.

Nature Chemical Biology: doi:10.1038/nchembio.2534